electronics

MDPI

Article

A Flexible and Pattern Reconfigurable Antenna with Small Dimensions and Simple Layout for Wireless Communication Systems Operating over 1.65–2.51 GHz

Adnan Ghaffar [1,*], Xue Jun Li [1], Wahaj Abbas Awan [2], Aqeel Hussain Naqvi [3], Niamat Hussain [4], Mohammad Alibakhshikenari [5,*] and Ernesto Limiti [5]

[1] Department of Electrical and Electronic Engineering, Auckland University of Technology, Auckland 1010, New Zealand; xuejun.li@aut.ac.nz
[2] Department of Integrated IT Engineering, Seoul National University of Science and Technology, Seoul 01811, Korea; wahajabbasawan@seoultech.ac.kr
[3] School of Electrical and Electronics Engineering, Chung-Ang University, Seoul 156756, Korea; aqeel2017110146@cau.ac.kr
[4] Department of Computer and Communication Engineering, Chungbuk National University, Cheongju 28644, Korea; hussain@chungbuk.ac.kr
[5] Electronic Engineering Department, University of Rome "Tor Vergata", Via Del Politecnico 1, 00133 Rome, Italy; limiti@ing.uniroma2.it
* Correspondence: aghaffar@aut.ac.nz (A.G.); alibakhshikenari@ing.uniroma2.it (M.A.)

Citation: Ghaffar, A.; Li, X.J.; Awan, W.A.; Naqvi, A.H.; Hussain, N.; Alibakhshikenari, M.; Limiti, E. A Flexible and Pattern Reconfigurable Antenna with Small Dimensions and Simple Layout for Wireless Communication Systems Operating over 1.65–2.51 GHz. *Electronics* **2021**, *10*, 601. https://doi.org/10.3390/electronics10050601

Academic Editor: Dimitra I. Kaklamani

Received: 25 January 2021
Accepted: 26 February 2021
Published: 4 March 2021

Abstract: This research article proposes a compact frequency and pattern reconfigurable flexible antenna for heterogeneous applications. A triangular monopole antenna with a semicircular stub is made frequency and pattern tunable by connecting and disconnecting two inverted L-shaped stubs utilizing diodes. When either of the stubs is connected to the radiator, a relative phase difference happens at both ends of the radiator that changes the direction of the electromagnetic radiations, consequently pattern reconfigurability can be obtain. Besides that, because of the reactive load introduced by the stubs, the antenna's effective length has changed and, as a result, the frequency reconfigurability can be attained. The antenna features a compact size of $40 \times 50 \times 0.254$ mm^3 corresponding to $0.22\lambda_o \times 0.27\lambda_o \times 0.001\lambda_o$, where λ_o is free-space wavelength at 1.65 GHz, while its operational bandwidth is from 1.65 GHz to 2.51 GHz, with an average gain and radiation efficiency of better than 2.2 dBi and 80%, exhibiting a pattern reconfigurability of 180° in the *E*-plane. The frequency of the proposed antenna can be switched from 2.1 GHz to 1.8 GHz by switching the state of both diodes in OFF and ON-state, respectively. The fabricated prototype of the antenna is tested to verify its performance parameters. In addition, to validate the proposed design, it has been compared with prior arts in terms of the overall size, reconfigurability type, flexibility, radio frequency (RF) switch type used for reconfigurability, and frequency bandwidth. The proposed antenna provides smaller size with a large bandwidth coverage alongside with discrete RF switch type with the advantages of flexibility and both frequency and pattern reconfigurability. As a result, the proposed compact flexible and pattern reconfigurable antenna is a promising candidate for heterogeneous applications, including the global system for mobile (GSM) band (1800 and 1900 MHz) and industrial, scientific and medical (ISM) band (2.4 GHz) along with well-known cellular communication bands of 3G, 4G, and long term evolution (LTE) bands ranging from 1700–2300 MHz around the globe.

Keywords: flexible antenna; frequency reconfigurability; pattern reconfigurable; 3G; 4G

1. Introduction

Multifunctional antennas are getting significant attention to meet the requirements of sensing, radar, and various wireless communication systems. Moreover, multifunctional antennas reduce the overall number of antennas in the system, thus decreasing the undesired mutual coupling and setbacks related to larger antenna dimensions [1]. Reconfigurable antennas arise as one of the potential candidates of multifunctional communication and allow ease of integration of numerous radio networks into one platform. The common operational mode of the reconfigurable antennas is on-demand frequency, polarization, and pattern reconfigurability [2,3]. The various techniques deployed to achieve reconfigurability include electrical, material, and mechanical methods by utilizing PIN diodes, optical switches, metasurface, micro fluids, mechanical switches, and so on [4]. Besides that, researchers have put more effort to design compound type reconfigurable antennas where a combination of more than one reconfigurability could be found, e.g., a frequency and pattern reconfigurability or frequency and polarization reconfigurability at the same time [5–7].

On the other hand, the demand for wearable technology increases in modern communication system due to the many applications in daily life like wristwatches, fitness bands, augmented reality, and usage in medical appliance. The wearable devices are worn by a person and communicate with other devices by cellular connectivity. In medical applications, they are used to monitor the critical health conditions, e.g., sugar level, examine inner intestinal system, blood pressure, and the temperature of the body. Besides that, wearable devices can also be integrated into jackets, shoes, rain coat, and helmets in rescue and emergency response. Antenna is the main part of the wearable system, and they to their advantages of conformability, lightweight, and durability over rigid antennas. Therefore, a natural demand for flexible, planar compact antennas and easy integration with a modern, flexible device has emerged [8]. Moreover, the compact dimension of flexible devices and overcrowded band spectrum allocation for various wireless communications require flexible and reconfigurable antennas. In this context, numerous works have been reported in the literature. However, existing works have a set of larger dimensions along with the limit of only pattern reconfigurability [9–11] or frequency reconfigurability [12–15]. A frequency and polarization reconfigurable antennas without and with artificial magnetic conductors were explained in references [16] and [17], respectively. A radiation pattern and polarization reconfigurable antenna were explained in other studies [18,19]. A reconfigurable partially reflective surface antenna with biasing network was explained in [20]. A frequency and radiation pattern reconfigurable antenna based on the center-shorted technique is presented in [21]. Two groups of varactors diodes are used for tuning the frequency and switching between broadside and monopole-like radiation pattern. Another low profile hybrid reconfigurable antenna by using the pin diodes was proposed in [22]. An antenna array was designed in [23] for frequency and radiation pattern reconfiguration. An independent biasing voltage circuitry is designed for pattern reconfigurability. A compact frequency and radiation pattern reconfigurable antenna for wireless communications has been reported in [24]. Moreover, to cover the 5G band, a novel frequency and radiation pattern reconfigurable antenna is presented in a study [25]. The proposed antenna consists of two patches and the different states of the transistors are used to excite the antenna at the required frequency band. These hybrid reconfigurable antennas [21–25] have the drawbacks of rigid structure, larger antenna size, and complex biasing structure which limits their applications for flexible electronics. In a previous study [26], a frequency and radiation pattern reconfigurable antenna to cover 1.9 and 2.4 GHz bands was proposed. Although the proposed antenna is flexible, it has a complex antenna structure and used several PIN diodes to realize the switching states of the antenna.

In this article, a frequency and pattern reconfigurable antenna is designed and realized using diode biasing. Two inverted L-shaped stubs are imprinted on the top side of a triangular monopole antenna. By changing the state of diodes, these stubs can be electrically connected and disconnected with the radiator. When either of the stubs is connected to the radiator, a relative phase difference occurs at both ends of the radiator, which changes the direction of the electromagnetic radiations, thus pattern reconfigurability could be achieved. Moreover, due to the reactive load introduced by the stubs, the effective length of the antenna is changed and hence the frequency reconfigurability is achieved. A simple yet effective technique is exploited for these features.

The major contribution of the proposed work can be summarized as:

- A relatively compact and simple structured antenna is designed for frequency and pattern reconfigurability at the same time.
- The antenna utilizes only two pin diodes to switch between two narrow bands and a wideband along with pattern reconfigurability from omnidirectional to the directional pattern.
- The antenna offers good performance in both conformal and non-conformal conditions along with a good agreement between simulated and measured results.
- Comparison with state of the artwork states that the presented antenna overperforms the related works by providing an overall better performance, as depicted in Table 1.

Table 1. Comparison of the proposed work with the state-of-the-art works.

Reference	Antenna Size (mm^2)	Reconfigurable Type	Material Type	RF Switch Type	Frequency (GHz)
[9]	35 × 25	Radiation Pattern	Flexible	Discrete	2.4–2.48
[13]	50 × 33	Frequency	Flexible	Discrete	2.18–2.3.58
[15]	24 × 19	Frequency	Flexible	Discrete	2.4/3.8/5.6
[16]	59 × 31	Polarization and Frequency	Flexible	Discrete	2.36/3.64
[17]	89 × 83	Polarization and Frequency	Flexible	Discrete	2.45/3.3
[21]	85 × 85	Radiation Pattern and Frequency	Solid	Continuous	2.68–3.51
[22]	50 × 50	Frequency and Radiation Pattern	Solid	Discrete	4.5/4.8/5.2/5.8
[23]	151.5 × 160.9	Frequency and Radiation Pattern	Solid	Continuous	2.15–2.38
[24]	23 × 31	Frequency and Radiation Pattern	Solid	Discrete	3.1–6.8
[25]	112 × 52	Frequency and Radiation Pattern	Solid	18 NMOS transistor	28/38
This work	40 × 50	Frequency and Radiation Pattern	Flexible	Discrete	1.65–2.51

2. Antenna Geometry and Design Methodology

Figure 1a–c shows the top, back, and side view of the geometrical configuration of the proposed flexible and compound reconfigurable antenna. The antenna geometry is imprinted on the top side of the ROGERS 5880LZ substrate having a dielectric constant (ε_r) of 2.1 and tangent loss (tanδ) of 0.002, while the thickness (H) of the substrate is 0.254 mm. The antenna consists of a coplanar waveguide (CPW) fed semicircular patch of radius R connected with a triangular radiator. Next, two inverted L-shaped stubs having the longest arm length S_L, shortest arm length S_W and width S_G is connected to the triangular radiator using two RF pin diodes D_1 and D_2 by SKYWORKS© having model number SMP-1345 SC-79. Two capacitors C_1 and C_2 of 100 pF capacitance are inserted to block DC to flow towards the SMA connector. On the backside of the substrate, small biasing pads were engraved to provide the required voltage and current to switch the state of diodes, while the two inductors L_1 and L_2 of 68 nH were inserted to block unnecessary RF currents. The optimized parameters of the proposed antenna are as follow (unit: mm): W = 40; L = 50; h = 0.254; L_g = 18; W_g = 5; g = 0.5; W_F = 3; L_F = 5; w_1 = 24.1; w_2 = 2; L_1 = 21.3; L_2 = 5.

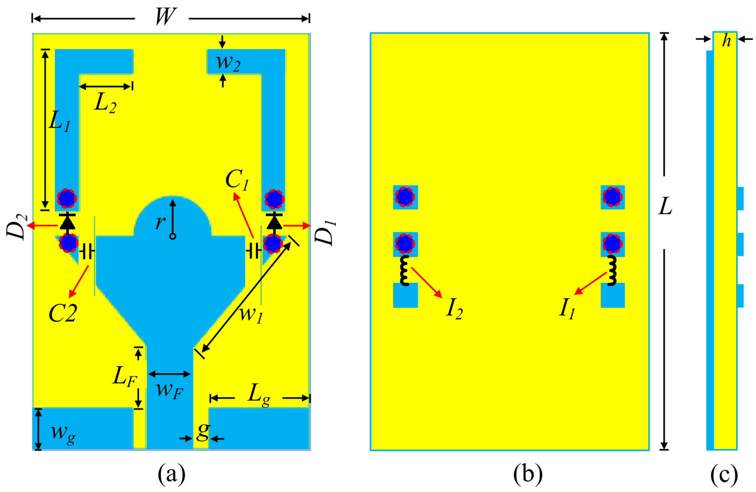

Figure 1. The geometry of the proposed antenna: (**a**) Front view, (**b**) back view, and (**c**) side view.

2.1. Design of the Compact Flexible Monopole Antenna

The proposed flexible antenna is originally derived from a conventional quarter-wave rectangular monopole antenna, the basic concept of the antenna designed methodology has been presented previously [27]. The resonating frequency of the monopole antenna can be estimated by using the following equation as given in [28].

$$f_r = \frac{c}{4L_o\sqrt{\varepsilon_{eff}}} \tag{1}$$

where c is the velocity of light, L_o is the effective length of the rectangular radiator, and ε_{eff} is the effective dielectric constant for $A/h < 1$, which can be computed as:

$$\varepsilon_{eff} = \frac{\varepsilon_r + 1}{2} + \frac{\varepsilon_r - 1}{2}\left\{\left(1 + 12\frac{h}{w}\right)^{-0.5} + 0.04\left(1 - \frac{w}{h}\right)^2\right\} \tag{2}$$

ε_r is the relative permittivity and h is the thickness of the substrate, while A is the width of the radiator. Next, to enhance the bandwidth of the conventional monopole, the lower edges of the radiator were truncated. The effects of truncation of the corner of the radiator on the performance of the antenna are well discussed in a study [29]. In the end, a semicircular patch having radius r is loaded with a triangular patch to provide an additional path for the flow of current, which consequently improved the impedance mismatching, as depicted in Figure 2.

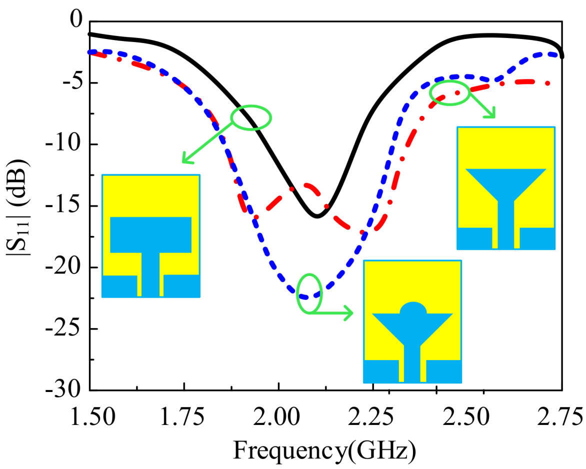

Figure 2. Extraction of the wideband antenna from conventional monopole.

2.2. Design of the Compound Reconfigurable Antenna

The flexible antenna designed above is further utilized to design a compound reconfigurable antenna by loading two inverted L-shaped stubs at the upper corners of the triangular radiator. The insertion of the stub at either end of the radiator generates a respective phase difference between two ends of the radiator, which resulted in pattern reconfigurability, as depicted in Figure 3. The phase difference (Φ) generated due to the presence of the stub can be calculated by:

$$\Phi \approx \frac{2\,\pi\,c\,L_T}{f} \tag{3}$$

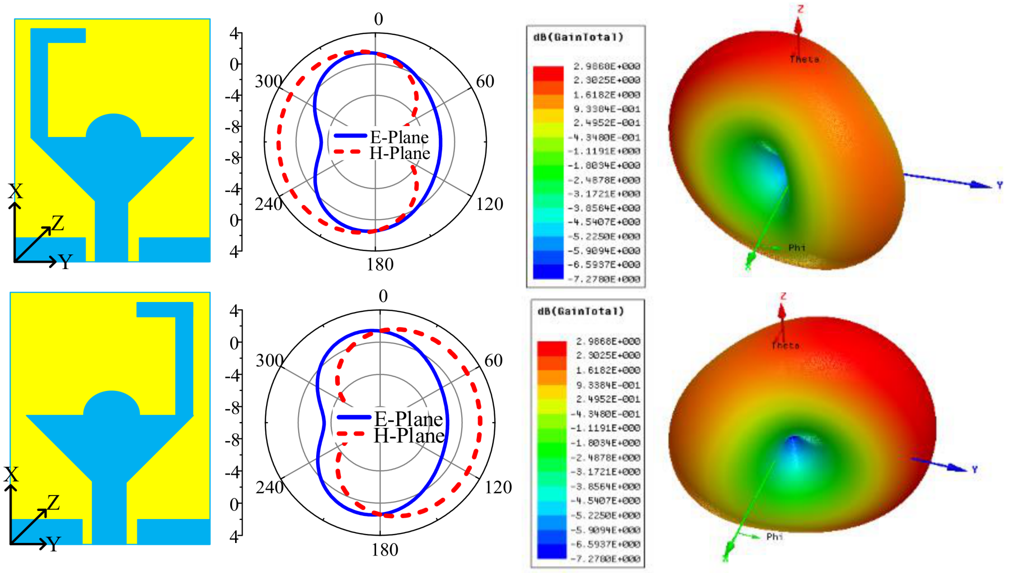

Figure 3. Effect of stub loading on the radiation patterns of the antenna.

Here, $\pi \approx \frac{22}{7}$, c is the velocity of light, f is the resonating frequency of the antenna, and L_T is the effective length of the stub, which can be calculated by:

$$L_T \approx L_1 + L_2 \tag{4}$$

Noteworthily, due to the insertion of the stub, the surface charges redistribute itself and flow more toward the stub, which forces the electromagnetic waves to propagate in a specific direction resulting in the deformation of the radiation pattern in that specific direction, as illustrated in Figure 3. Next, the reactance loaded at the one end of the radiator due to the insertion of the stub increases the effective area of the radiator, which results in the generation of additional resonance at a lower frequency, as depicted in Figure 4. Moreover, it is also observed that, when both ends were loaded with stubs, the maximum surface charge distribution is along with the stubs while less amount of charges are distributed on the triangular patch. Therefore, the resonance is mainly due to stubs, and the antenna starts representing only at a lower frequency. Then, two pin diodes are inserted between stubs and triangular patch to achieve on-demand frequency and pattern reconfigurability as shown previously in the final proposed design (See Figure 1).

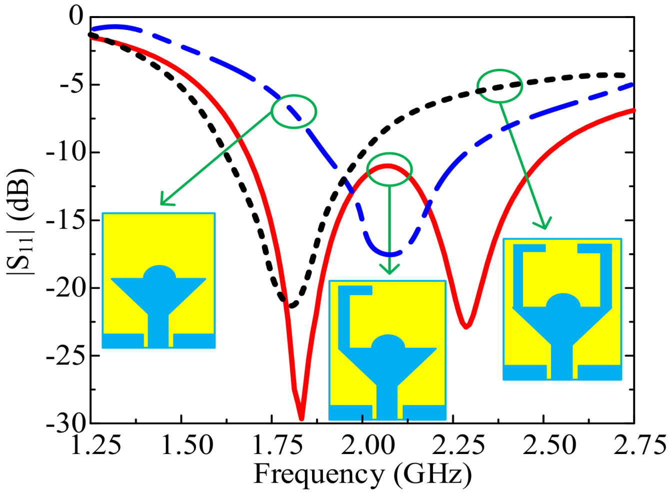

Figure 4. S-parameter comparison of various steps involved in antenna designing.

3. Results and Discussion

The simulation of the proposed antenna was done using higher frequency structure simulator (HFSS) electromagnetic solver. The equivalent electrical model of the diode was constructed by utilizing lumped elements in such a way that for ON-state, the diode behaves like a series combination of 0.7 *nH* inductor with 5 Ω resistor. While for OFF-state, the diode behaves like a series combination of 0.7 *nH* inductor along with a parallel combination of 5 kΩ resistor and 0.2 *pF* capacitor. Figure 5 illustrates the equivalent model of diode along with the biasing circuit use to provide pure DC-current to switch the state of the diode. Additionally, to validate the findings, a prototype of the proposed antenna is fabricated and tested as shown in Figure 6. The reflection coefficient of the proposed antenna was measured by a portable vector network analyzer (Anritsu S820E). The near-field characteristics of the antenna was measured through a commercial near-field measurement system in a shielded RF anechoic chamber by using antenna and propagation kit (ME1310) from Keysight Technologies. The horn antenna having a standard gain of 24 dBi is utilized as a transmitter, while the proposed antenna was measured as a receiving antenna. The signal generator was used to provide stable power reception. The antenna is rotated in 360° to measure the near-field results. The setup for the radiation pattern is shown in Figure 7.

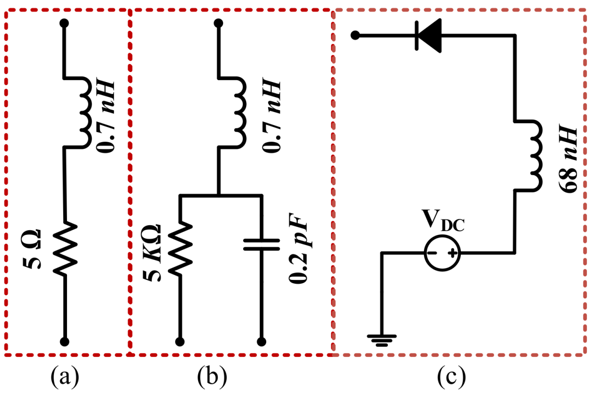

Figure 5. Equivalent model of diode for (**a**) ON-state, (**b**) OFF-state, and (**c**) biasing circuit.

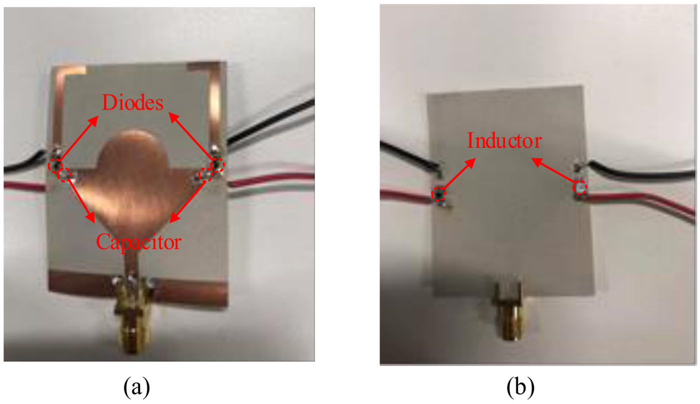

Figure 6. Fabricated prototype of the proposed flexible antenna: (**a**) Top-view and (**b**) bottom view.

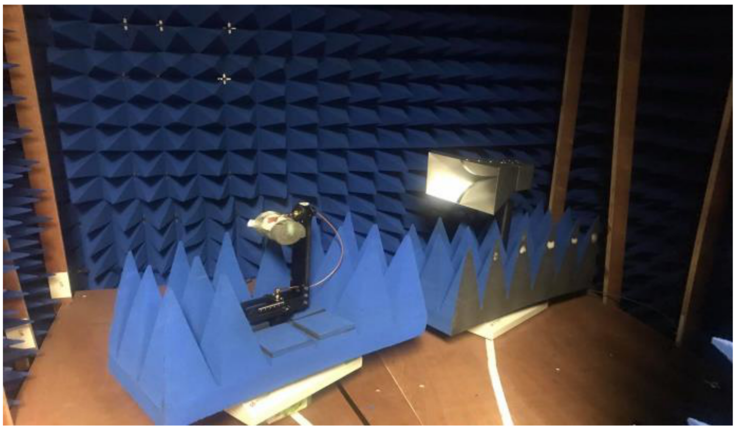

Figure 7. Antenna measurement setup.

3.1. Reflection Coefficient

Figure 8 presents the simulated and measured reflection coefficient of the proposed antenna for different switching cases of the diode. For case-00 (both diodes are in OFF-state), the simulated results show that the antenna exhibits an impedance bandwidth of 410 MHz (1.91–2.32 GHz), while the measured results show that the antenna exhibits impedance bandwidth of 480 MHz ranging from 1.81–2.29 GHz. When either of the diode D_1 or D_2 is OFF (case-01 or case-10), a simulated impedance bandwidth of 830 MHz (1.68–2.51 GHz) is achieved. On the other hand, the measured value for case-01 is noted to be 910 MHZ (1.64–2.55 GHz), and that for case-10 was 920 MHz ranging 1.635–2.555 GHz. The minor variation between case-01 and case-10 is due to imperfect fabrication and measurement system. For case-00 (both diodes are in OFF-state), the antenna starts resonating at 1.8 GHz having simulated and measured impedance bandwidth of 400 MHz (1.65–2.05 GHz) and 460 MHz (1.63–2.09 GHz), respectively. In general, a good agreement among simulated and measured scattering parameter results was observed due to less effect of the biasing circuit as it is printed on the backside of the substrate.

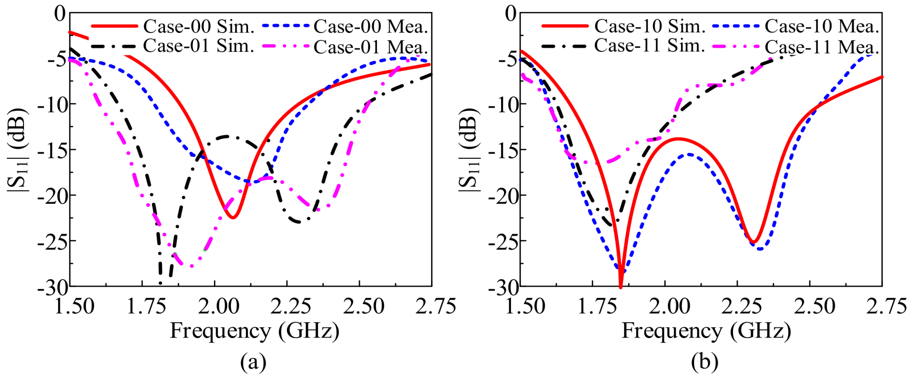

Figure 8. Simulated and measured reflection coefficient responses (S11<–10 dB) of the proposed antenna for different switching cases of the diode, (**a**) case–00, case–01; (**b**) case–10, case–11.

3.2. Conformability Analysis

For any flexible device, the antenna should maintain characteristics for non-conformal and conformal conditions; therefore, the presented antenna is bent along *X*-axis, and *Y*-axis and its characteristics are analyzed. For simulation purposes, the antenna is wrapped on a cylinder of radius 25 mm chosen keeping in mind that the edges of the antenna do not touch each other (Figure 9a). For measurements, a flexible foam having a similar radius was chosen and the fabricated prototype was attached to it, as depicted in Figure 9b. The S-parameters of the antenna with different switching states under the conformal condition are shown in Figure 10a–d. A strong agreement along simulated and measured results was observed for all switching states. Moreover, the similar results for conformal and non-conformal conditions state the potential of proposed work for both rigid and flexible devices.

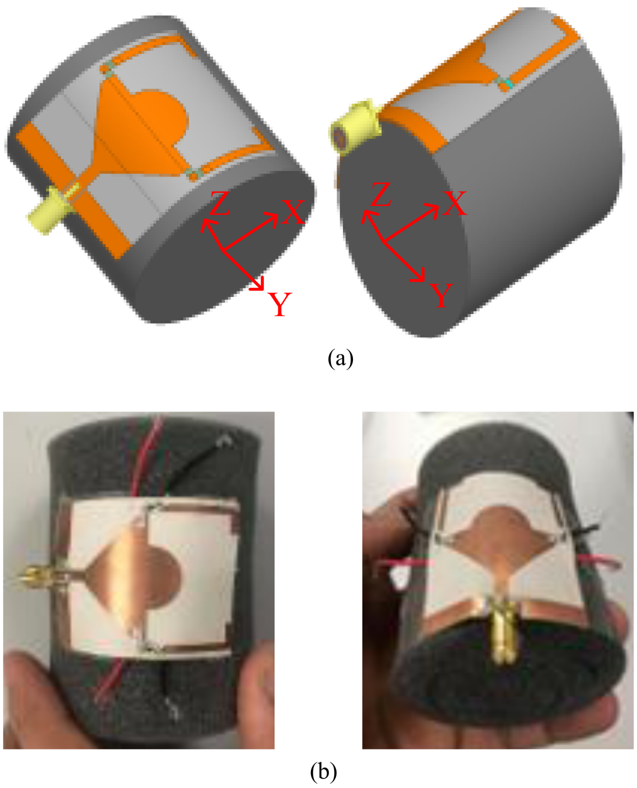

Figure 9. System of the structure used for conformability analysis: (**a**) Simulation setup and (**b**) measurement setup.

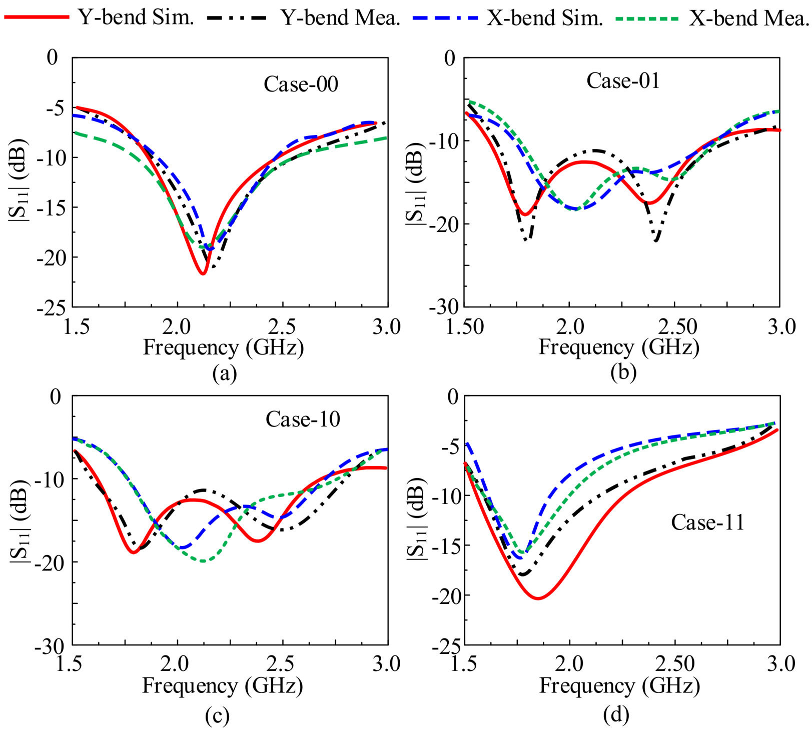

Figure 10. S-parameters for the antenna with different switching states under bending conditions (**a**) case–00; (**b**) case–01; (**c**) case–10; (**d**) case–11.

3.3. Near-Field Analysis of Conformal and Non-Conformable Antenna

Figure 11 presents the comparison among simulated and measured radiation patterns of the antenna for possible switching states of diodes at various frequencies. It can be observed from Figure 11a,b that for case-00 (at 2.1 GHz) and case-11 (at 1.8 GHz), the antenna exhibits omnidirectional radiation pattern in principle *E*-plane (Φ = 0°), and a bi-directional radiation pattern is observed in *H*-plane (Φ = 90°). The radiation pattern of the proposed antenna gets deviated from the original form and points toward +90° and −90° as depicted in Figure 10c,d, respectively.

Figure 12 presents the radiation pattern of the proposed antenna under bend condition along the *X*-axis and *Y*-axis. For brevity, only the measured results of case-01 and case-10 were reported at the selected frequency of 2.1 GHz. When being bent along *Y*-axis, the antenna exhibits identical results as of without bending. On the other hand, when the antenna was bent along *X*-axis, a little deviation is observed, as depicted in Figure 11c,d, which is mainly due to a large variation in the flow of current when the antenna was bent along the *X*-axis.

In general, the antenna exhibits a good agreement between simulated results for both conformal and non-conformal cases, which confirms the stability of the proposed work, thus making it a potential candidate for both conformal and non-conformal applications.

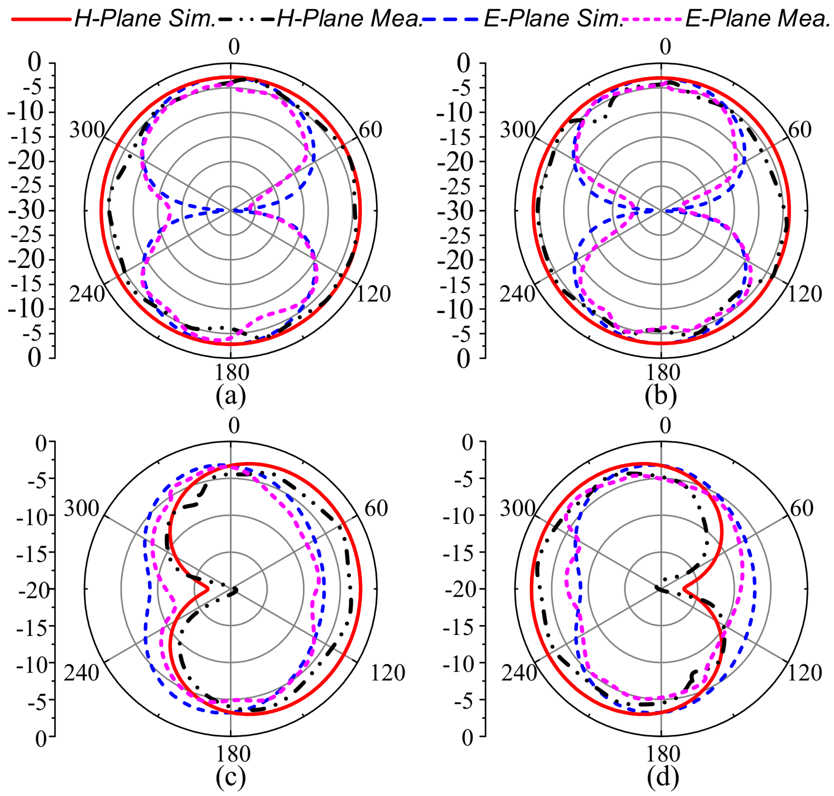

Figure 11. Comparison among simulated and measured radiation patterns (**a**) 2.1 GHz [case-00]; (**b**) 1.8 GHz [case-11]; (**c**) 2.1 GHz [case-01]; (**d**) 2.1 GHz [case-10].

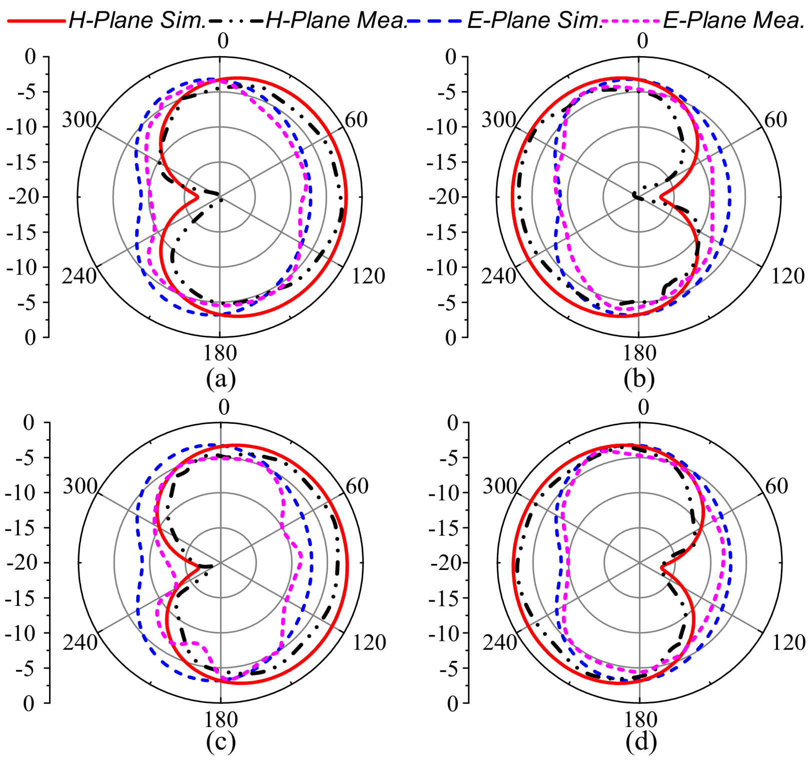

Figure 12. Comparison among simulated and measured radiation patterns of the antenna under bend condition at 2.1 GHz (**a**) bend along *Y*-axis [case-10], (**b**) bent along *Y*-axis, [case-01] (**c**) bent along *X*-axis [case-10], and (**d**) bent along *X*-axis [case-01].

3.4. Gain and Radiation Efficiency

The gain and radiation efficiency of the proposed antenna for case-00, case-01, case-10, and case-11 are presented in Figure 13. It could be observed that the average value of the simulated and measured gain for all cases is better than 2.2 dBi over the operational bandwidth, while for non resonating bands, gain tend to start decreasing. Furthermore, it is observed that the antenna offers the average radiation efficiency of more than 80% for all pass bands of each case.

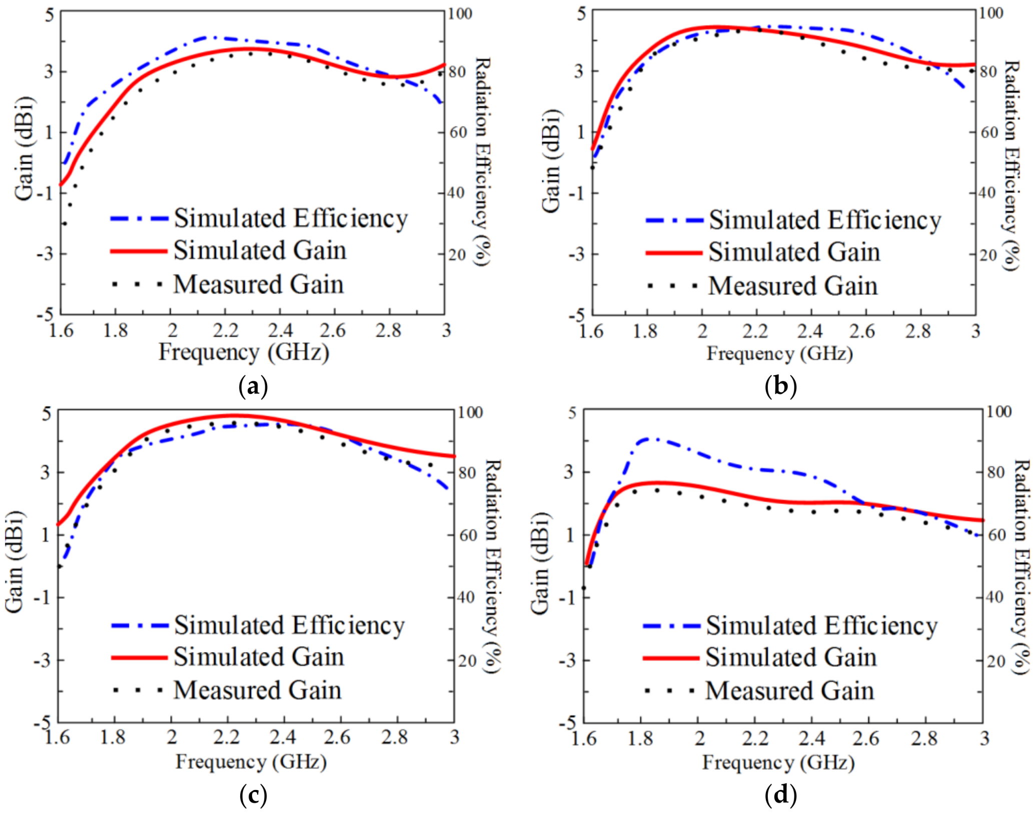

Figure 13. Radiation gain and efficiency curves over the frequency band of proposed antenna for (**a**) case-00, (**b**) case-01, (**c**) case-10, and (**d**) case-11.

3.5. Comparison with State-of-the-Art Works

The performances of the proposed antenna (in terms of overall size, reconfigurability type, flexibility, RF switch type used for reconfigurability, and frequency bandwidth) have been compared with state-of-the-art antennas. The antenna overperforms the reported antennas due to its smaller size, discrete RF switch type with the advantages of flexibility, and both frequency and pattern reconfigurability.

4. Conclusions

This paper presents a hybrid frequency and pattern reconfigurable antenna. The geometrical structure of the proposed antenna consists of a semicircular patch loaded on a triangular radiator along with two inverted *L*-shaped stubs, which are utilized to achieve compound reconfigurability using diodes. The antenna comprises a simple structure along with a compact size of $40 \times 50 \times 0.254$ mm^3 correspond to $0.22\lambda_o \times 0.27\lambda_o \times 0.001\lambda_o$, where λ_o is free-space wavelength at 1.65 GHz. The frequency of the proposed antenna can be switched from 2.1 GHz to 1.8 GHz by switching the state of both diodes in OFF and ON-state, respectively. Moreover, when one diode is in ON-state while keeping the other in OFF-state, the antenna shows a wide impedance bandwidth of 1.65–2.5 GHz along with tilted radiation patterns in the *E*-plane. The strong agreement between simulated and measured results for both conformal and non-conformal conditions makes the proposed work a promising candidate for the applications like wearables and medical related devices operating in 3G, 4G, LTE, GSM, and ISM bands.

Author Contributions: Conceptualization, A.G., W.A.A., and M.A; methodology, W.A.A., N.H., and M.A.; software, A.G., W.A.A., and N.H.; validation, A.H.N., X.J.L., M.A., and E.L.; investigation, A.H.N. N.H., and M.A.; resources, N.H., A.G., and M.A.; writing—original draft preparation, W.A.A., N.H., and A.G.; writing—review and editing, A.H.N., X.J.L., M.A., and E.L.; supervision, X.J.L. All authors have read and agreed to the published version of the manuscript.

Funding: This research received no external funding.

Data Availability Statement: Data is contained within the article.

Conflicts of Interest: The authors declare no conflict of interest.

References

1. Le, T.T.; Park, H.-Y.; Yun, T.-Y. Simple Reconfigurable Circularly Polarized Antenna at Three Bands. *Sensors* **2019**, *19*, 2316. [CrossRef]
2. Naqvi, A.H.; Lim, S. Microfluidically polarization-switchable metasurfaced antenna. *IEEE Antennas Wirel. Propag. Lett.* **2018**, *17*, 2255–2259. [CrossRef]
3. Awan, W.A. A Miniaturized Wideband and Multi-band On-Demand Reconfigurable Antenna for Compact and Portable Devices. *AEU-Int. J. Electron. Commun.* **2020**, *2020*, 153266. [CrossRef]
4. Parchin, N.O.; Basherlou, H.J.; Al-Yasir, Y.I.; Abd-Alhameed, R.A.; Abdulkhaleq, A.M.; Noras, J.M. Recent developments of reconfigurable antennas for current and future wireless communication systems. *Electronics* **2019**, *8*, 128.
5. Li, K.; Shao, Z.H.; Wang, Q.; Cheng, Y.J. Frequency-and pattern-reconfigurable antenna for multistandard wireless applications. *IEEE Antennas Wirel. Propag. Lett.* **2014**, *14*, 333–336. [CrossRef]
6. Liu, J.; Li, J.; Xu, R. Design of very simple frequency and polarisation reconfigurable antenna with finite ground structure. *Electron. Lett.* **2018**, *54*, 187–188. [CrossRef]
7. Lin, W.; Wong, H.; Ziolkowski, R.W. Circularly polarized antenna with reconfigurable broadside and conical beams facilitated by a mode switchable feed network. *IEEE Trans. Antennas Propag.* **2017**, *66*, 996–1001. [CrossRef]
8. Mohamadzade, B.; Simorangkir, R.B.; Maric, S.; Lalbakhsh, A.; Esselle, K.; Hashmi, R.M. Recent Developments and State of the Art in Flexible and Conformal Reconfigurable Antennas. *Electronics* **2020**, *9*, 1375. [CrossRef]
9. He, X.; Gao, P.; Zhu, Z.; You, S.; Wang, P. A flexible pattern reconfigurable antenna for WLAN wireless systems. *J. Electromagn. Waves Appl.* **2019**, *33*, 782–793. [CrossRef]
10. Tang, M.-C.; Zhou, B.; Duan, Y.; Chen, X.; Ziolkowski, R.W. Pattern-reconfigurable, flexible, wideband, directive, electrically small near-field resonant parasitic antenna. *IEEE Trans. Antennas Propag.* **2018**, *66*, 2271–2280. [CrossRef]
11. Chen, S.L.; Qin, P.Y.; Lin, W.; Guo, Y.J. Pattern-reconfigurable antenna with five switchable beams in elevation plane. *IEEE Antennas Wirel. Propag. Lett.* **2018**, *17*, 454–457. [CrossRef]
12. Hussain, N. A Compact Flexible Frequency Reconfigurable Antenna for Heterogeneous Applications. *IEEE Access* **2020**, *8*, 173298–173307. [CrossRef]
13. Saraswat, K.; Harish, A.R. Flexible dual-band dual-polarised CPW-fed monopole antenna with discrete-frequency reconfigurability. *IET Microw. Antennas Propag.* **2019**, *13*, 2053–2060. [CrossRef]
14. Yang, S.; Vaseem, M.; Shamim, A. Fully Inkjet-Printed VO2-Based Radio-Frequency Switches for Flexible Reconfigurable Components. *Adv. Mater. Technol.* **2019**, *4*, 1800276. [CrossRef]
15. Sreelakshmi, K.; Rao, G.S.; Kumar, M.N.V.S.S. A Compact Grounded Asymmetric Coplanar Strip-Fed Flexible Multiband Reconfigurable Antenna for Wireless Applications. *IEEE Access* **2020**, *8*, 194497–194507. [CrossRef]
16. Saeed, S.M.; Balanis, C.A.; Birtcher, C.R. Inkjet-printed flexible reconfigurable antenna for conformal WLAN/WiMAX wireless devices. *IEEE Antennas Wirel. Propag. Lett.* **2016**, *15*, 1979–1982. [CrossRef]
17. Saeed, S.M.; Balanis, C.A.; Birtcher, C.R.; Durgun, A.C.; Shaman, H.N. Wearable flexible reconfigurable antenna integrated with artificial magnetic conductor. *IEEE Antennas Wirel. Propag. Lett.* **2017**, *16*, 2396–2399. [CrossRef]
18. Raman, S.; Mohanan, P.; Timmons, N.; Morrison, J. Microstrip-fed pattern-and polarization-reconfigurable compact truncated monopole antenna. *IEEE Antennas Wirel. Propag. Lett.* **2013**, *12*, 710–713. [CrossRef]
19. Row, J.S.; Kuo, L.K. Pattern-Reconfigurable Array Based on a Circularly Polarized Antenna with Broadband Operation and High Front-to-Back Ratio. *IEEE Trans. Antennas Propag.* **2019**, *68*, 4109–4113. [CrossRef]
20. Ji, L.Y.; Guo, Y.J.; Qin, P.Y.; Gong, S.X.; Mittra, R. A reconfigurable partially reflective surface (PRS) antenna for beam steering. *IEEE Trans. Antennas Propag.* **2015**, *63*, 2387–2395. [CrossRef]
21. Nguyen-Trong, N.; Hall, L.; Fumeaux, C. A frequency-and pattern-reconfigurable center-shorted microstrip antenna. *IEEE Antennas Wirel. Propag. Lett.* **2016**, *15*, 1955–1958. [CrossRef]
22. Selvam, Y.P.; Kanagasabai, M.; Alsath, M.G.; Velan, S.; Kingsly, S.; Subbaraj, S.; Rao, Y.R.; Srinivasan, R.; Varadhan, A.K.; Karuppiah, M. A low-profile frequency-and pattern-reconfigurable antenna. *IEEE Antennas Wirel. Propag. Lett.* **2017**, *16*, 3047–3050. [CrossRef]

23. Zainarry, S.N.M.; Nguyen-Trong, N.; Fumeaux, C. A frequency-and pattern-reconfigurable two-element array antenna. *IEEE Antennas Wirel. Propag. Lett.* **2018**, *17*, 617–620. [CrossRef]
24. Iqbal, A.; Smida, A.; Mallat, N.K.; Ghayoula, R.; Elfergani, I.; Rodriguez, J.; Kim, S. Frequency and pattern reconfigurable antenna for emerging wireless communication systems. *Electronics* **2019**, *8*, 407. [CrossRef]
25. Shereen, M.K.; Khattak, M.I.; Al-Hasan, M.A. A Frequency and Radiation Pattern Combo-Reconfigurable Novel Antenna for 5G Applications and Beyond. *Electronics* **2020**, *9*, 1372. [CrossRef]
26. Zhu, Z.; Wang, P.; You, S.; Gao, P. A flexible frequency and pattern reconfigurable antenna for wireless systems. *Prog. Electromagn. Res.* **2018**, *76*, 63–70. [CrossRef]
27. Ghaffar, A.; Li, X.J.; Hussain, N.; Awan, W.A. Flexible Frequency and Radiation Pattern Reconfigurable Antenna for Multi-Band Applications. In Proceedings of the 4th IEEE Australian Microwave Symposium (AMS), Sydney, Australia, 13–14 February 2020; pp. 1–2.
28. Balanis, C.A. *Antenna Theory: Analysis and Design*; John Wiley & Sons: Hoboken, NJ, USA, 2016.
29. Abbas, A. A rectangular notch-band UWB antenna with controllable notched bandwidth and centre frequency. *Sensors* **2020**, *20*, 777. [CrossRef]